



DOI: 10.34910/MCE.109.1

## Effect of elastomer polymer on the moisture susceptibility of asphalt concrete

A. Shabani<sup>a</sup> , Gh.H. Hamed<sup>b</sup> \* 

<sup>a</sup> KTH Royal Institute of Technology, Stockholm, Sweden

<sup>b</sup> University of Guilan, Rasht, Guilan Province, Iran

\*E-mail: [hamedi@guilan.ac.ir](mailto:hamedi@guilan.ac.ir)

**Keywords:** experimental investigations, strength, moisture, cyclic loads, asphalt mixtures, asphalt pavements, polymers

**Abstract.** There are various experimental methods for improving the moisture strength of asphalt concrete, such that the most common one being the use of anti-stripping materials. In the present paper, the influences of polymer materials on asphalt binder were investigated using repetitive loading test in wet and dry conditions along with thermodynamic parameters based on the surface free energy (SFE) components of asphalt binder and aggregates. The obtained results of this investigation indicate that using styrene butadiene rubber (SBR) polymer has improved the asphalt concrete strength against the moisture damage, especially in the specimens made of granite aggregates. Also, SBR polymer increases the cohesion free energy and reduces the energy released by the system during the stripping event, which represents a decrease in the tendency for stripping. The stripping percentage index, which is obtained by combining the results of the repetitive loading test in wet and dry conditions along with the results of thermodynamic parameters, represents that the specimens made of controlled asphalt binder in the loading cycles under wet conditions have a higher stripping rate. Also, the modulus loss rate in control asphalt concrete is faster than the modified specimens.

### 1. Introduction

Aggregates and asphalt binder are two main components of asphalt concrete as a composite material [1]. Asphalt binder is absorbed on the surface of aggregates and forms the asphalt binder film. This film sticks aggregates to each other and creates the strong structure of asphalt mixture [2]. Displacement of asphalt binder from the aggregate surface or failure in the asphalt binder film is defined as moisture damage. This type of damage occurs when the aggregates have a greater tendency to absorb water than being coated by the asphalt binder [3]. In addition to moisture damage, moisture causes different damages such as rutting, fatigue, shoving, bleeding, and pothole [4].

In order to compare the susceptibility and the effects of stripping additives and the moisture damage potential of asphalt concrete, a variety of experimental tests have been performed in wet and dry conditions [5]. The modified Lottman method (AASHTO T283) is a well-known experimental approach in this field which does not focus on the fundamental properties of materials that effects on damage event, and they cannot present the reason for the weakness or the strength of asphalt concrete [6]. Accordingly, in the last two decades, many studies have been conducted on using different methods based on the properties of materials that affect the asphalt binder cohesion and the asphalt binder-aggregate adhesion for determination of the moisture susceptibility of asphalt concrete.

---

Shabani, A., Hamed, Gh.H. Effect of elastomer polymer on the moisture susceptibility of asphalt concrete. Magazine of Civil Engineering. 2022. 109(1). Article No. 10901. DOI: 10.34910/MCE.109.1

© Shabani, A., Hamed, Gh.H., 2022. Published by Peter the Great St. Petersburg Polytechnic University.



This work is licensed under a CC BY-NC 4.0

## 1.1. Previous studies

Free energy of asphalt mixture constituent elements play a significant role in mechanical properties of asphalt concrete [7]. The primary investigation was reported in Texas Transportation Institute by Elphinstone [8], which revealed that SFE measurements could be applied as an impressive tool to predict moisture damage and fatigue cracking in asphalt concrete. Cheng [9] examined the concepts of SFE and its application in asphalt concrete. The results of his study showed that thermodynamic changed in adhesion and cohesion of SFE were directly related to debonding in the asphalt binder aggregates' contact surface and cracks in the mastic. Abandansari and Modarres [10] investigated the influence of using nanomaterials on moisture strength of asphalt concrete by using mechanical and thermodynamic methods. Bhasin [11] initially developed the methods to measure the SFE components of asphalt binder and aggregate. Then, he investigated the relationship between the thermodynamic parameters, which were obtained by measuring the SFE components of asphalt binders and aggregates as well as the moisture susceptibility potential in the asphalt concrete. Following the previous studies, Howson [12] evaluated using SFE for identification of the resistance of asphalt concrete against moisture. The obtained experimental results of this investigation indicated that the modifications made on asphalt binder had negative or positive influences on their SFE components and adhesion energy. In the study reported by Moghadas Nejad and Hamedei [13], the relationship between moisture damage potential and thermodynamic parameters was evaluated using the susceptibility test results from different combinations of asphalt concrete. The results showed that the thermodynamic parameters were significantly associated with the event and severity of moisture damage [14].

In recent years polymer and nanomaterial have also been applied to investigate the moisture properties of asphalt concrete [15, 16]. The most important methods for improving the asphalt mixture's strength against moisture are changing the mixture design, materials, or using anti-stripping additives. Changes in the mix design can also slightly affect the asphalt mixture strength against moisture. Accordingly, using anti-stripping additives is the most optimal method to improve the asphalt mixture's strength against moisture [17]. Although studies have been carried out on an aggregate modification to improve asphalt mixture's strength against moisture, most of these studies have been limited to experimental studies [18, 19]. Hydrated lime [20], nano anti-stripping [21], and liquid anti-stripping [22] additives are the most common anti-stripping materials used in the experimental studies and executive projects.

## 1.2. SFE theory

SFE of the materials has been described in several theories according to the molecular structure. An acidic-basic theory is one of the most significant theories which is used extensively for the description of the SFE components of various materials [23].

By combining the mentioned components, the total SFE can be obtained as the following expression:

$$\Gamma = \Gamma^{LW} + \Gamma^{AB}. \quad (1)$$

Hitherto,  $\Gamma$ ,  $\Gamma^{AB}$ , and  $\Gamma^{LW}$  denote the total SFE of the materials, the polar component of SFE, and the non-polar component of SFE, respectively.  $\Gamma^{AB}$  can be explained as Equation (2) which is a composition of Lewis acid ( $\Gamma^+$ ) and base components ( $\Gamma^-$ ).

$$\Gamma^{AB} = 2\sqrt{\Gamma^+\Gamma^-}. \quad (2)$$

From the thermodynamic perspective, the cohesion free energy ( $\Delta G_i^c$ ) can be explained as the amount of energy required for creating a crack in a material with the unit surface. Based on this definition, the total cohesion work is obtained for different materials as Equation (3):

$$W^{AC} = 2\Gamma_A, \quad (3)$$

where  $\Gamma_A$  denotes the total SFE of the desired material. Cohesion work of an asphalt binder is a significant factor applied in some fracture mechanics basic equations to determine the energy required to grow tiny cracks in the asphalt binder phase or the asphalt mixture mastic phase.

Adhesion free energy ( $\Delta G_i^a$ ) is defined based on two main components of non-polar or Lifshitz Van der Waals ( $\Delta G_i^{aAB}$ ) and Polar or acid-base ( $\Delta G_i^{aLW}$ ). Hence, Equation (4) is applied for the determination of the adhesion-free energy between aggregate and asphalt binder.

$$\Delta G_i^a = -W^a = \Delta G_i^{aLW} + \Delta G_i^{aAB} = -2 \left[ \left( \sqrt{\Gamma_2^{lw} \Gamma_1^{lw}} \right) + \left( \sqrt{\Gamma_2^+ \Gamma_1^-} \right) + \left( \sqrt{\Gamma_2^- \Gamma_1^+} \right) \right], \quad (4)$$

where  $\Gamma_1^{lw}$ ,  $\Gamma_1^+$  and  $\Gamma_1^-$  are the asphalt binder components' SFE and  $\Gamma_2^{lw}$ ,  $\Gamma_2^+$  and  $\Gamma_2^-$  are the aggregate components' SFE. For a mixture of aggregate and asphalt binder, Equation (4) is used for the case when the SFE components of the mixture are measured.

From a thermodynamic point of view, the  $\Delta G_i^c$  is the total work per unit area to form two new surfaces, the energy of which is equal to the sum of the surface energies of the two newly created surfaces. In addition, the  $W^a$  is the work required to separate two materials at their contact surface under vacuum conditions. The cohesion and adhesion works are shown in Fig. 1.

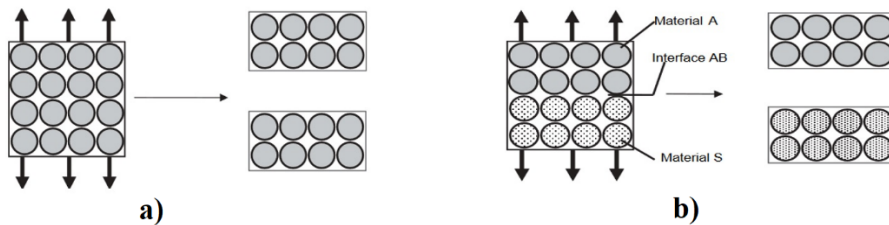


**Figure 1. a – the cohesion, b – the adhesion work of energy.**

Equation (5) is used to calculate aggregate and asphalt binder adhesion in the presence of water. In this equation, the subscripts of 1, 2, and 3 show the asphalt binder, aggregate, and water, respectively. It is noteworthy to mention that the negative values of adhesion free energy represent that the two materials tend to bond with each other. For the case when the  $\Delta G_i^a$  value becomes more negative, this tendency increases.

$$\Delta G_{132}^a = \Gamma_{12} - \Gamma_{13} - \Gamma_{23} = - \left[ \begin{array}{l} \left( 2\Gamma_3^{LW} \right) + \left( 4\sqrt{\Gamma_3^+ \Gamma_3^-} \right) - \left( 2\sqrt{\Gamma_1^{LW} \Gamma_3^{LW}} \right) \\ - \left( 2\sqrt{\Gamma_3^+ \Gamma_1^-} \right) - \left( 2\sqrt{\Gamma_1^+ \Gamma_3^-} \right) - \left( 2\sqrt{\Gamma_2^{LW} \Gamma_3^{LW}} \right) \\ - \left( 2\sqrt{\Gamma_3^+ \Gamma_2^-} \right) - \left( 2\sqrt{\Gamma_2^+ \Gamma_3^-} \right) - \left( 2\sqrt{\Gamma_1^{LW} \Gamma_2^{LW}} \right) \\ + \left( 2\sqrt{\Gamma_1^+ \Gamma_2^-} \right) + \left( 2\sqrt{\Gamma_2^+ \Gamma_2^-} \right) \end{array} \right]. \quad (5)$$

### 1.3. Problem statement and research objectives

Although the currently-used anti-stripping materials have reduced moisture damage in asphalt concrete, their use is associated with a series of executive or technical problems [23]. Therefore, this research has attempted to investigate the use of polymer modifiers. Also, despite the numerous studies conducted on the application of thermodynamic methods in detecting the susceptibility of asphalt concrete, it is worth mentioning that its use as a tool to determine the susceptibility of different asphalt concrete and its effects on the anti-stripping mechanism has not yet been widespread. Therefore, this study attempts to first obtain the SFE components of the controlled and modified asphalt binder and aggregate. The most significant objectives of the present study can be categorized as follows:

1. Studying the influence of SBR polymer on the controlled asphalt binder's SFE components

2. Studying the influence of SBR polymer on thermodynamic parameters including asphalt binder-aggregate adhesion free energy, asphalt binder cohesion free energy, and the system's free energy in the event of stripping
3. Studying the effects of using SBR polymer on the modulus ratio of wet to dry condition in the controlled and modified specimens
4. Comparing the results of the thermodynamic parameters and modulus ratio in wet to dry conditions
5. Combining the results of the thermodynamic parameters and repetitive loading to determine the process of stripping event in the controlled and modified specimens.

## 2. Methods

### 2.1. Designing an experimental program

Different experimental procedures used in this study include:

1. Modifying the controlled asphalt binder with SBR in two different percentages;
2. Mix design by AASHTO T245 method;
3. Implementing the repetitive loading test on specimens made of controlled and modified asphalt binders;
4. Determining the SFE components of the controlled and modified asphalt binders using Wilhelmy plate and Universal Sorption Device (USD);
5. Calculating thermodynamic parameters based on SFE components of asphalt binders, aggregates, and water for various compounds of asphalt concrete, and;
6. Calculating the percentage of asphalt concrete' aggregate surface stripping in different loading cycles by combining the results of repetitive loading test and thermodynamic parameters.

### 2.2. Materials

#### 2.2.1. Aggregate

In the present paper, two different types of granite and limestone aggregates have been used, which are acidic and basic, respectively. The main reason for using these two different aggregates is the different structure of minerals constituting these two types of aggregates, which makes them different in their susceptibility to moisture damage. The structure of aggregate surface minerals is evaluated by the X-ray fluorescence (XRF) experiment. The results of these experiments are presented in Table 1.

**Table 1. Structure of minerals forming aggregates used in this study.**

Properties	Limestone	Granite
Calcium oxide, CaO (%)	72.47	31.75
Magnesium oxide, MgO (%)	2.24	2.92
Ferric oxide, Fe <sub>2</sub> O <sub>3</sub> (%)	3.87	7.08
Aluminum oxide, Al <sub>2</sub> O <sub>3</sub> (%)	4.84	1.74
Silicon dioxide, SiO <sub>2</sub> (%)	13.58	52.19

The gradation of aggregates used in the present investigation is the ASTM-standard medium grading to produce dense asphalt concrete. The rated size of the aggregates in this gradation is 19 mm [24]. The aggregate gradations of two used materials are illustrated in Fig. 2, whereas their physical properties are documented in Table 2.

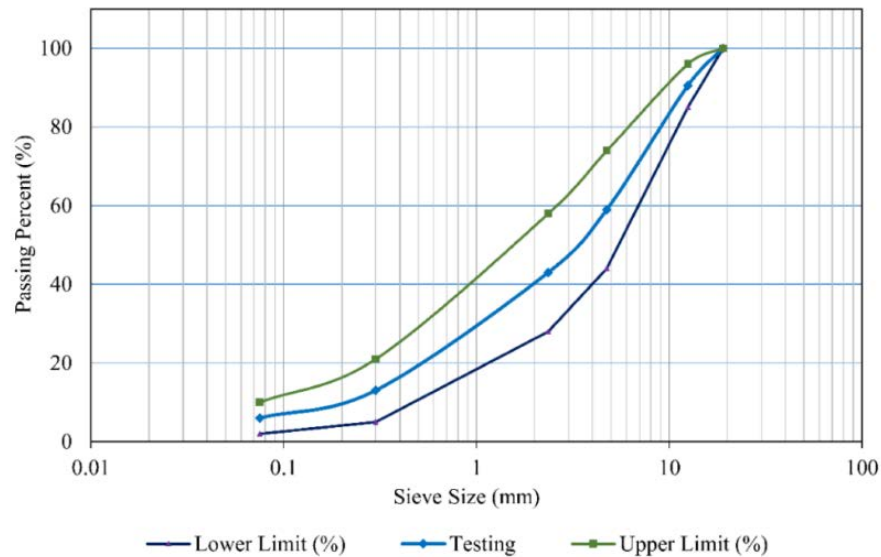


**Figure 2. Gradation of aggregates used in this study.**

**Table 2. Physical properties of aggregates used in this study.**

Properties	Standard	Limestone	Granite	Specification limit
Coarse aggregate				
Bulk specific gravity (g/cm <sup>3</sup> )	ASTM C 127	2.63	2.61	–
SSD specific gravity (g/cm <sup>3</sup> )		2.65	2.63	–
Apparent specific gravity (g/cm <sup>3</sup> )		2.68	2.67	–
Fine aggregate				
Bulk specific gravity (g/cm <sup>3</sup> )	ASTM C 128	2.62	2.60	–
SSD specific gravity (g/cm <sup>3</sup> )		2.65	2.62	–
Apparent specific gravity (g/cm <sup>3</sup> )		2.68	2.65	–
Specific gravity of filler (g/cm <sup>3</sup> )	ASTM D 854	2.65	2.65	–
Los Angeles abrasion (%)	ASTM C 131	32	22	Max 45
Flat and elongated particles (%)	ASTM D 4791	9	6	Max 10
Sodium sulfate soundness (%)	ASTM C 88	7	9	Max 10–20
Fine aggregate angularity	ASTM C 1252	56.2	59.2	Min 40

### 2.2.2. Asphalt binder

The base asphalt binder used in the present paper has the penetration grade of 60–70 provided by the Isfahan refinery. Table 3 presents the characteristics of the asphalt binder. The asphalt binder is modified by SBR polymer materials in two different percentages. The next section will explain the anti-stripping materials used in this study and their properties.

**Table 3. Properties of base asphalt binders used in this study.**

Properties	Standard	Value
Penetration (mm/10)	ASTM D5-73	69
Softening point (°C)	ASTM D36-76	51
Ductility (cm)	ASTM D113-79	105
Flashpoint (°C)	ASTM D92-78	262
Loss of heating (%)	ASTM D1754-78	0.75
Trichloroethylene solubility, (%)	ASTM D2042-76	99.5

### 2.2.3. SBR polymer

SBR describes a family of synthetic rubbers that consist of styrene and butadiene. These materials have a suitable strength against wear and aging. SBR is defined as a common polymer with high efficiency, and it is considered to be the world's most consumed rubber, due to the availability of cheap and abundant raw materials. Therefore, it has the highest volume of production in the rubber industry [25]. The mechanical properties of the SBR polymer used in this study are presented in Table 4.

**Table 4. Mechanical properties of the SBR polymer used in this study.**

Properties	Value
Tensile Strength (MPa)	18
Elongation at tear (%)	544
Mooney Viscosity (100 °C)	49.2
Glass transition temperature (°C)	-60
Polydispersity	2.7
PH	9.5

## 2.3. Laboratory Studies

### 2.3.1. Asphalt binder modification

In this study, SBR polymer material is used as an anti-stripping asphalt binder modifier. This material is used at 2 and 4 % of asphalt binder weight. For the production of modified asphalt binders, the base asphalt binder is first heated to 160 °C, and then the additives are added at the intended percentage. Mixing operation is carried out in the mixer at the rate of 2000 rpm for 15 minutes. Since mixing procedure causes aging in asphalt binder [26], the base asphalt binder is placed in the mixer at the same conditions to experience the effect of aging similar to the modified asphalt binders.

### 2.3.2. Mix design

In the present investigation, the Marshall mix design has been applied according to the AASHTO T245 standard for the determination of the optimum asphalt binder content [27]. Also, the optimum asphalt binder content is determined based on the MS-2 guideline of the Asphalt Institute. The values of optimum asphalt binder were calculated based on the average asphalt binder content corresponding to the maximum unit weight, maximum Marshall stability, and 4 % air void. The corresponding values of the five parameters of Marshall stability, flow, air void (AV), voids in mineral aggregate (VMA), and void fill with asphalt binder (VFA) were then controlled by the specifications.

### 2.3.3. Repetitive loading test

The repetitive load test was used to determine the modulus of asphalt concrete in dry and wet conditions. The AASHTO T283 method is used to subject the specimens to wet conditions. The modified AASHTO T283 method is one of the most common methods used to determine moisture sensitivity of HMA. It should be considered that the percentage of existing air pores of the mixture should be 6.5–7.5 %. Three cases of prepared specimens are remained in dry conditions and the other 3 specimens should be conditioned in order to prepare wet specimens. First, the specimens should be saturated using relative vacuum conditions under absolute pressure of 13–67 kPa for 5 minutes. Samples are then kept submerged without vacuum conditions for 5–10 minutes, and in the following, specimens are withdrawn and weighted in order to achieve the saturation percent of 70–80 %. Then the specimens are kept into freezer at -18 °C for 16 h and after that the specimens are placed in warm water bath at 60 °C and they are allowed to remain at this temperature for 24 h. In this study, the indirect tensile modulus experiment is conducted at 25 °C and a frequency of 1 Hz under haversine loading with the stress level of 300 kPa. The value of the indirect tensile modulus for each mixture in a particular loading cycle can be measured by using Equation (6).

$$E^* = \frac{\sigma_{\max}}{\epsilon_{\max}}, \quad (6)$$

where  $\sigma_{\max}$  is the maximum stress for a particular cycle and  $\epsilon_{\max}$  is the corresponding stress in the same cycle.

Modulus ratio for each cycle is obtained according to Equation (7), which is considered as an indicator for moisture susceptibility in asphalt concrete [28]. The larger the parameter  $K$  is, according to

Equation (7), means that the asphalt mixture strength against the simultaneous effects of traffic and high moisture is higher.

$$K = \frac{E_{wet}^*}{E_{dry}^*} \times 100, \quad (7)$$

where,  $E_{wet}^*$  and  $E_{dry}^*$  indicate the indirect tensile modulus value in wet and dry conditions, respectively.

#### 2.3.4. Measuring the SFE components of aggregate and asphalt binder

A variety of methods can be used to measure the SFE components of asphalt binder and aggregate. Due to the susceptibility of measurement in these experiments, the methods used here are the methods that were proven to have higher accuracy in the previous studies [29].

##### 2.3.4.1. Measuring the SFE components of aggregates

Universal Sorption Device (USD) has been used to measure the aggregate's SFE indirectly using gas adsorption by three solvents. Hence, for the creation of a set of three equations and three unknowns (the three components of the solid matter's SFE), three equations are needed. Therefore, it could be noted that three research matters, whose SFE components should be specified, are required for calculation of the SFE components of a solid body.

The relationship between the vapor pressure of a vapor of the probe material and the mass of a vapor absorbed on the surface of an aggregate is an example of isothermal adsorption. Moreover, the relationship between the adhesion work and the square root of the SFE components (Equation 8) is linear. Therefore, three equations are required to create a set of three equations with three unknowns, with each equation needing a probe material. Thus, three probe materials are required to obtain the SFE components of a solid.

$$W_{S,V}^a = \pi_e + 2\Gamma_v^{total} = -2 \left[ \sqrt{\Gamma_s^{LW} \Gamma_l^{LW}} + \sqrt{\Gamma_s^+ \Gamma_l^-} + \sqrt{\Gamma_s^- \Gamma_l^+} \right], \quad (8)$$

where  $W_{S,V}^a$  is the work of adhesion between the surface aggregate (S) and vapor (V),  $\Gamma_V^{Total}$  is the total SFE of liquids tested, and  $\pi_e$  is the equilibrium pressure distribution of the liquid vapor over the aggregate surface.

USD is able to indirectly obtain the SFE components of the aggregate using three different probe liquids. Generally, the passing aggregates of 4.75 mm and the residue on sieve 2.36 mm are used. 40 g of these aggregates are washed and dried on a 2.36 mm sieve to remove dust and moisture completely. Finally, these aggregates are washed using water, methanol, hexane and again methanol. After washing is complete, these aggregates are brought to standard room temperature. Once the materials have reached room temperature (25 °C), they are placed inside the aluminum mesh sample holder of the USB device.

The equilibrium pressure distribution on the aggregate is obtained as Equation 9:

$$\pi_e = \frac{RT}{MA} \int_0^p \frac{pn}{p} dp. \quad (9)$$

In which  $R$  is the gas constant,  $T$  is the test temperature (Kelvin),  $M$  is the molecular mass of the tested vapor-liquid,  $n$  is the mass of the absorbed vapor per unit mass of the aggregate at vapor pressure  $p$ , and  $A$  is the specific surface area of the aggregate, which is calculated as follows using the BET equation (Equation 10):

$$A = \left( \frac{n_m \times N_0}{M} \right) \times \alpha, \quad (10)$$

where  $N_0$  is Avogadro's number,  $\alpha$  is the imaged surface of one molecule, and  $n_m$  is single-layer capacity. The number of molecules required to cover the surface of the aggregate in one layer is referred to as the absorbable monolayer capacity on the aggregate surface, which can be obtained by Equation 11. In this equation,  $S$  and  $I$  denote the slope and intercept of the diagram between  $p/n(p_0 - p)$  and

$p/p_0$ ,  $P$  stands for the partial vapor pressure,  $P_n$  indicates the saturated vapor pressure, and  $n$  represents the mass of the absorbed vapor relative to the aggregate mass.

$$n_m = \frac{1}{s + I}. \quad (11)$$

The SFE components for different used materials are reported in Table 5.

**Table 5. SFE components of the research materials for measuring the SFE components of aggregates (ergs/cm<sup>2</sup>).**

SFE components	SFE components (ergs/cm <sup>2</sup> )				
	Total SFE	Lifshitz Van der Waals	Polar	Acidic	Basic
n-Hexane	18.4	18.4	0	0	0
Methyl Propyl Ketone (MPK)	24.7	24.7	0	0	19.6
Water	72.8	21.8	51	25.5	25.5

#### 2.3.4.2. Measuring SFE components of asphalt binder

In this section, the Wilhelmy plate technique is used to obtain the contact angle between the asphalt binder and a liquid which is a characteristic of the hydrophilicity or hydrophobicity of the surface [30].

The relationship between the vapor pressure of a vapor of the probe material and the mass of a vapor absorbed on the surface of an aggregate is an example of isothermal adsorption. Moreover, the relationship between the adhesion work and the square root of the SFE components (Equation 12) is linear. Therefore, three equations are required to create a set of three equations with three unknowns, with each equation needing a probe material. Thus, three probe materials are required to obtain the SFE components of a solid.

$$W_{S,V}^a = \pi_e + 2\Gamma_v^{total} = -2 \left[ \sqrt{\Gamma_s^{LW} \Gamma_l^{LW}} + \sqrt{\Gamma_s^+ \Gamma_l^-} + \sqrt{\Gamma_s^- \Gamma_l^+} \right], \quad (12)$$

where  $W_{S,V}^a$  is the work of adhesion between the surface aggregate ( $S$ ) and vapor ( $V$ ),  $\Gamma_v^{total}$  is the total SFE of liquids tested, and  $\pi_e$  is the equilibrium pressure distribution of the liquid vapor over the aggregate surface.

USD is able to indirectly obtain the SFE components of the aggregate using three different probe liquids. Generally, the passing aggregates of 4.75 mm and the residue on sieve 2.36 mm are used. 40 g of these aggregates are washed and dried on a 2.36 mm sieve to remove dust and moisture completely. Finally, these aggregates are washed using water, methanol, hexane and again methanol. After washing is complete, these aggregates are brought to standard room temperature. Once the materials have reached room temperature (25 °C), they are placed inside the aluminum mesh sample holder of the USB device.

The equilibrium pressure distribution on the aggregate is obtained as Equation 13:

$$\pi_e = \frac{RT}{MA} \int_0^{P_n} \frac{n}{p} dp, \quad (13)$$

where  $R$  is the gas constant,  $T$  is the test temperature (Kelvin),  $M$  is the molecular mass of the tested vapor-liquid,  $n$  is the mass of the absorbed vapor per unit mass of the aggregate at vapor pressure  $p$ , and  $A$  is the specific surface area of the aggregate, which is calculated as follows using the BET equation (Equation 14):

$$A = \left( \frac{n_m \times N_0}{M} \right) \times \alpha, \quad (14)$$

where  $N_0$  is Avogadro's number,  $\alpha$  is the imaged surface of one molecule, and  $n_m$  is single-layer capacity. The number of molecules required to cover the surface of the aggregate in one layer is referred to as the absorbable monolayer capacity on the aggregate surface, which can be obtained by Equation 15.



In this equation,  $S$  and  $I$  denote the slope and intercept of the diagram between  $p/n(p_0 - p)$  and  $p/p_0$ ,  $P$  stands for the partial vapor pressure,  $P_n$  indicates the saturated vapor pressure, and  $n$  represents the mass of the absorbed vapor relative to the aggregate mass.

$$n_m = \frac{1}{s+1}. \quad (15)$$

To obtain the passive components, at least three fluids with specified surface energy components are required. In this paper, water, formamide, and glycerin have been used due to the relatively large amounts of SFE components, non-miscible with asphalt binder, and different amounts of SFE. Their surface energy components are provided in Table 6.

**Table 6. SFE components of the research materials for measuring the SFE components of asphalt binder (ergs/cm<sup>2</sup>).**

SFE components	SFE components (ergs/cm <sup>2</sup> )				
	Total SFE	Lifshitz Van der Waals	Polar	Acidic	Basic
Water	72.6	21.6	51	25.5	25.5
Glycerol	62.8	34	28.8	3.92	57.4
Formamide	58	39	19	2.28	39.6

### 3. Results and Discussion

#### 3.1. Mix design

The optimum asphalt binder content in the specimens made of granite and limestone aggregates was 5.5 and 5.8 %, respectively. Due to their surface porosity, limestone aggregates absorb more asphalt binder. This process causes more optimum asphalt binder content to be absorbed compared to the granite aggregates with fewer pores.

It should be mentioned that the mix design is only carried out for specimens containing aggregates and base asphalt binders, because if different asphalt binder percentages are used in the specimens containing controlled and modified asphalt binders, the asphalt binder content variable is also an important factor affecting the modulus ratio in wet to dry condition which causes the results to face an error.

#### 3.2. SFE tests

##### 3.2.1. Measuring the SFE components of aggregates

Table 7 indicates the results of measuring the SFE components of aggregates used in the present paper. In all reported cases, the basic components of both aggregates are higher than their acidic components. However, as it is clear, the ratio of the acidic to the basic component of granite aggregate is higher than the limestone aggregate. The non-polar component of limestone and granite aggregates are close to each other, but the polar component of limestone aggregate is more than granite aggregate, which has led to a significant increase in the total SFE associated with limestone aggregate compared to granite aggregate.

**Table 7. The SFE components of aggregates used in this study.**

Aggregate type	SFE components (ergs/cm <sup>2</sup> )				
	Basic	Acidic	Polar	Nonpolar	Total
Limestone	522.4	31.7	257.5	67.1	324.6
Granite	525.8	20.5	207.7	68.8	276.6

##### 3.2.2. Measuring the SFE components of asphalt binders

Asphalt is a single-phase homogeneous mixture of many different molecules, which may be differentiated into two broad classes: polar and non-polar. The non-polar molecules serve as a matrix or solvent for the polar molecules, which form weak "networks" of polar-polar associations that give asphalt its elastic properties. The polar materials are uniformly distributed throughout the asphalt, and upon heating the weak interactions are broken to yield a Newtonian fluid. Asphalts that have too much polar material will

be subject to fatigue cracking in thin pavements, brittleness, and thermal cracking. Asphalts that have too much non-polar material, or asphalts in which the non-polar materials are too low in molecular weight, will suffer from fatigue cracking in thick pavements, moisture sensitivity, and rutting. Asphalt binder is acidic in nature. Results related to the controlled and modified asphalt binder's SFE are presented in Table 8. As is clear from the table data, the base asphalt binder's acidic component is higher than its basic component. This causes the asphalt binder to have more acidic properties. Acidic properties of asphalt binder lead to the formation of stronger bonds with basic materials such as lime aggregates. The use of SBR polymer has increased both the acid and basic components of modified asphalt binders. The percentage of increase in the basic component is higher than the acidic component, which results in the formation of more basic properties in the SBR modified asphalt binders. An increase in the percentage of this material from 2 to 4 percent also increases the mentioned changes.

The results of Table 8 show that SBR polymer has increased the asphalt binder polar component. The positive or negative impact of this parameter on the asphalt binder-aggregate adhesion cannot be stated with certainty. The only thing to mention is that the increase in the polar properties of asphalt binders will increase their adhesion tendency to polar materials such as aggregate and water.

The results related to a non-polar component of asphalt binder's SFE in Table 8 show that using SBR polymer has increased the non-polar component of modified asphalt binders compared to the base asphalt binder. This leads to a formation with stronger non-polar bonds.

The total SFE results show that using SBR polymer has increased this parameter. The total SFE has a direct and linear relationship with cohesion free energy. The increase in the total SFE increases cohesion free energy. This means that higher energy is needed for the creation of a specific crack on the asphalt binder film. Increasing the energy needed for failure in the asphalt binder film reduces the probability of cohesion failure.

**Table 8. SFE components of controlled and modified asphalt binders used in this study.**

Asphalt binder type	SFE components (ergs/cm <sup>2</sup> )				Total SFE
	Basic	Acidic	Polar	Nonpolar	
AC 60/70	0.45	2.69	2.20	11.36	13.56
AC 60/70 with 2 % SBR	0.79	2.98	3.07	12.28	15.35
AC 60/70 with 4 % SBR	1.03	3.27	3.67	13.84	17.51

### 3.2.3. Thermodynamic parameters

Results related to the cohesion free energy parameters, debonding energy, and adhesion free energy have been provided in Fig. 3–5.

A closer look in Fig. 3 shows that using SBR polymer has increased cohesion free energy value. This suggests that higher energy is required for cracking on the asphalt binder film which reduces the probability of cohesion failure.

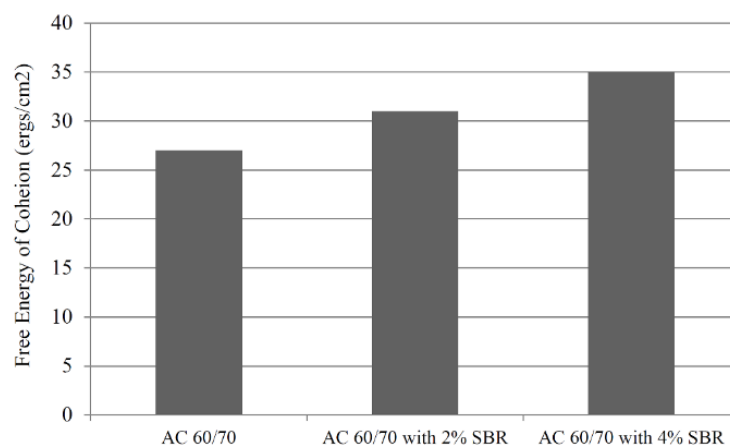


**Figure 3. Cohesion free energy in controlled and modified asphalt binders.**

Results related to the asphalt binder-aggregates adhesion free energy in dry conditions are shown in Fig. 4. This parameter presents the amount of energy required for creation of failure in asphalt binder-aggregate contact surface. It means that more energy is needed for separation of the asphalt binder from the aggregate surface. The amount of adhesion free energy in the specimens made of granite aggregate is more considerable than limestone aggregate. This suggests that more energy is required to separate the asphalt binder from the granite aggregate surface unit.

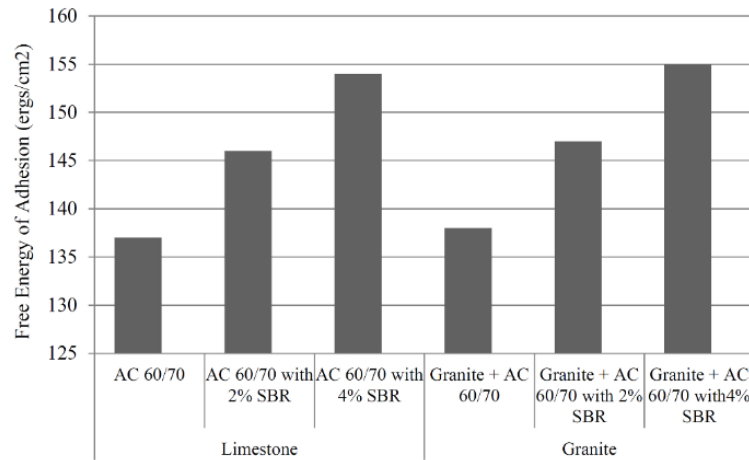


**Figure 4. The asphalt binder-aggregate adhesion free energy under dry conditions.**

According to the principles of thermodynamics, any energizer process is performed spontaneously. Therefore, when water enters into the binder-aggregate system, the asphalt binder debonding and the stripping event are expected to happen spontaneously. The important thing here is that greater amounts of released energy, lead to a higher stripping intensity. The results presented in Fig. 5 show that the use of SBR polymer in the specimens made of both types of aggregates has reduced the debonding energy. Increasing the percentage of these materials has reduced the value of this parameter. So, increasing the percentage of the polymer material has increased the tendency for stripping. As the data provided in the figure suggests, in the stripping of the compounds made of granite aggregates more energy is released, which indicates that stripping in the granite aggregate surface unit is more likely to occur.

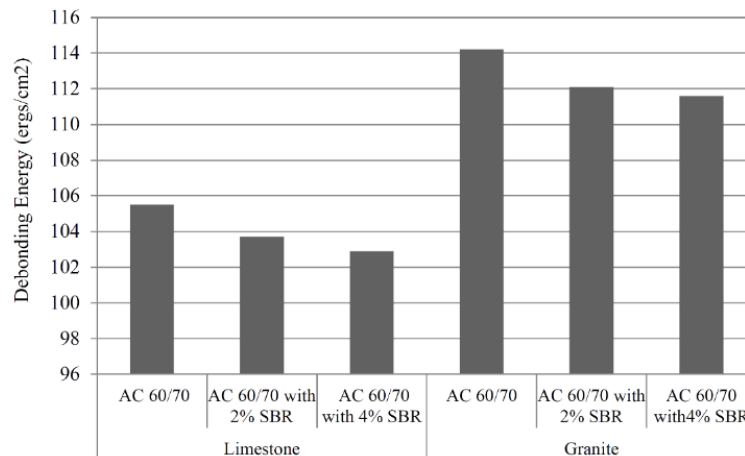


**Figure 5. The asphalt binder-aggregate adhesion free energy under wet conditions.**

### 3.3. Repetitive loading tests

Modulus ratio results for the specimens made of limestone and granite aggregates have been provided in Fig. 6, 7. The obtained results in Fig. 6, 7 shows the obvious effects of using the aggregates, asphalt binders and different additives on the moisture damage. Each of these components with mixed features can strengthen or weaken the asphalt mixture against moisture damage.

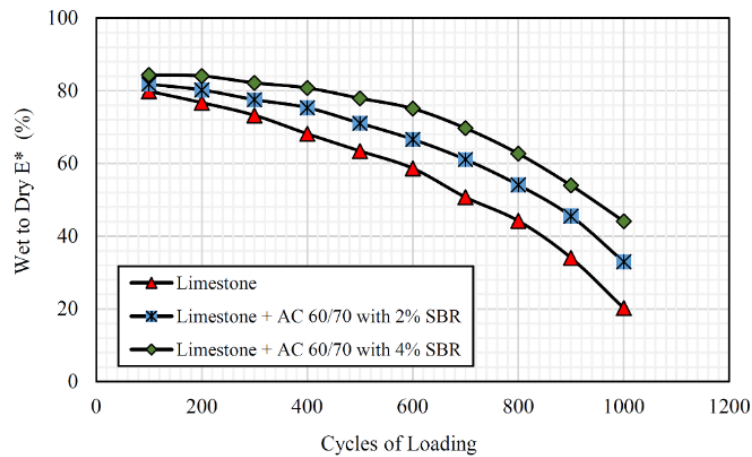


**Figure 6. Indirect tensile modulus ratio in samples made of limestone aggregates.**

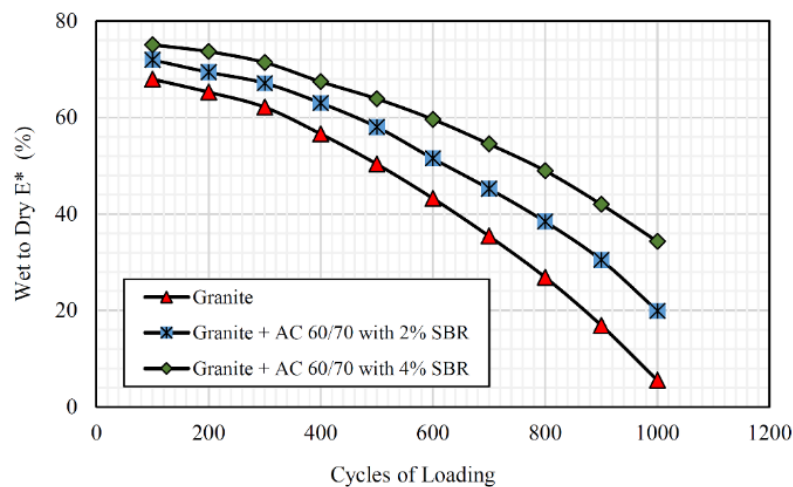


**Figure 7. Indirect tensile modulus ratio in samples made of granite aggregates.**

According to the results obtained in Fig. 6, the specimens made of controlled asphalt binder have the lowest modulus ratio in wet to dry conditions. The use of SBR polymer has increased the modulus ratio in these specimens. By increasing the percentage of the polymer additive, better performance of asphalt mixture against moisture has become more evident. The difference in the ratio of wet to dry modulus in the low loading cycle has become lower between the controlled and modified specimens. As the number of loading cycle increases, this difference also increases. In fact, it can be noted that the rate of decrease in the modulus (slope) in the controlled specimens is higher than the modified specimens.

The similar trend observed in specimens made of limestone aggregate can be seen in the specimens made of granite aggregate. The notable difference is that the use of SBR additives has made more improvements to the specimens made of granite aggregate.

As was observed in the analysis of the SFE method's results, the use of polymer materials increases cohesion and adhesion free energy in dry conditions. These two events reduce failure in the asphalt binder-aggregate contact surface and asphalt binder film, which increases the asphalt mixture's strength in loading conditions. As expected, placing the specimens under wet conditions has reduced asphalt mixture's strength against loading, because the influences of moisture reduce cohesion in asphalt binder and cause loss of adhesion in asphalt binder-aggregates. All of these factors reduce the asphalt mixture's strength.

### 3.4. Stripping percentage of the aggregates in loading cycles

Cheng [9] successfully used the continuous non-linear viscoelastic theory provided by Schapery for material damage for the description of the response of asphalt concrete under the strain and stress control loading. He applied the Schapery theory which mentioned that damage prediction was validated by repetitive loading tests based on diffusion theory. Thus, the moisture damage of asphalt concrete is obtained in repetitive loading by calculation of the aggregate surface percentage, which is subjected to stripping in different cycles. As can be observed in Equation (16), the strength ratio (modulus) in wet to dry conditions can be considered to be same as the adhesion ratio between aggregates-asphalt binder in wet and dry conditions [31].

$$\frac{E_{*wet}}{E_{*dry}} = \frac{[\Delta G_{12} * (1 - P) + \Delta G_{132} P]}{[\Delta G_{12}]}, \quad (16)$$

where  $\Delta G_{12}$  denotes the asphalt binder-aggregate adhesion energy,  $\Delta G_{132}$  denotes the asphalt binder-aggregate debonding or system energy in a saturated condition, and  $P$  is the percentage of the aggregate surface which is subjected to stripping.

For repetitive loading test of strain control, Equation (16) can be converted to Equation (17).

$$\frac{E_{*wet}}{E_{*dry}} = \frac{\left(\frac{\sigma}{\varepsilon}\right)_{wet}}{\left(\frac{\sigma}{\varepsilon}\right)_{dry}} = \frac{\varepsilon_{wet}}{\varepsilon_{dry}} = \frac{[\Delta G_{12} (1 - P) + \Delta G_{132} P]}{[\Delta G_{12}]}. \quad (17)$$

All parameters of Equation (17), except for index  $P$ , can be obtained from the thermodynamic concepts by measuring the SFE components of asphalt binders and aggregates (Tables 7, 8) and wet to dry modulus ratio (Fig. 6, 7). Knowing that  $P$  is the only thing missing from this equation, it can be calculated and used to determine the stripping trend of the aggregate surface from asphalt binders in different loading cycles for various asphalt concrete.

Results related to asphalt binder stripping percentage from the aggregate surface on the specimens made of granite and limestone aggregates are provided in Fig. 8, 9, respectively. As a consequence, using polymer additives has reduced the asphalt binder stripping percentage from the aggregate's surface in different loading cycles. Moreover, it can be observed that the slope in the stripping percentage against the loading cycles chart has an increasing trend. In fact, all aggregates in the primary cycles of loading are attached to the asphalt binder. Higher exposure of specimens to wet conditions and loading frequency leads to a higher percentage of aggregates to be stripped from the asphalt binder. This causes the adhesion reduction and the attached aggregate percentage reduction to intensify each other, and therefore, the asphalt binder stripping from the aggregate surface continues with a steeper slope.

It can be observed from Fig. 8, 9 that specimens made of limestone aggregates have higher strength compared to the specimens made of granite aggregates. Different factors are effective in the occurrence of moisture damage and the strength of asphalt concrete against it. The structure of minerals forming the aggregates used in asphalt concrete is one of the most significant parameters. Two minerals,  $\text{SiO}_2$ , and  $\text{CaO}$  (or  $\text{CaCO}_3$ ) cause a significant change in the hydrophobic or hydrophilic properties of aggregates. A higher percentage of  $\text{SiO}_2$  mineral indicates that the hydrophilic tendency of aggregates has increased and vice versa.

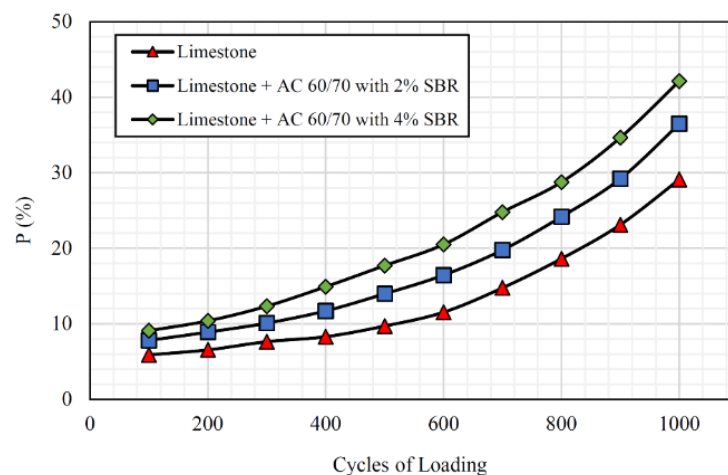
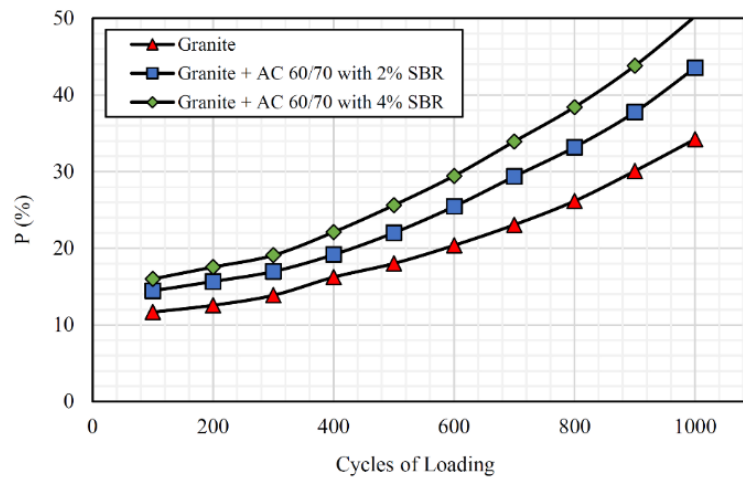


Figure 8. Stripping percentage of aggregate surface in samples made of limestone aggregates.



**Figure 9. Stripping percentage of aggregate surface in samples made of granite aggregates.**

Conversely, a higher percentage of the CaO mineral indicates that the hydrophobic tendency of aggregates has increased and vice versa [32]. It can be observed from Table 1 that a large part of granite aggregate is formed by silicon dioxide ( $\text{SiO}_2$ ) which leads to strong acidic properties. The amount of strong basic parts such as calcium oxide (CaO) in this type of aggregate is much lower than the acidic part. There are hydroxyl groups (OH) on the surface of granite aggregate. These groups (SiOH) form hydrogen bonds with carboxylic acids, which are very effective in asphalt binder-aggregates adhesion. However, hydrogen bond easily breaks in the presence of water, and these two groups are separated, and each one produces a hydrogen bond with water molecules [33]. Conversely, in the case of limestone aggregates, it is observed that the  $\text{SiO}_2$  mineral percentage is much lesser than the CaO mineral. In fact, the main reason for the high adhesion strength between limestone aggregates and asphalt binders is caused by the formation of insoluble bonds (covalent) in water that is formed due to the physical reaction between the calcium on the aggregate surface and some functional groups of asphalt binder.

#### 4. Conclusions

There are various experimental methods for improving the moisture susceptibility in asphalt concrete, and the most common one is the use of anti-stripping additives. Technical and executive problems of the existing anti-stripping materials and the technical defects in the moisture susceptibility evaluation methods of asphalt concrete have led to the study of the SBR polymer effects using mechanical and thermodynamic techniques. The most important experimental results obtained in the present investigation are:

1. Using SBR polymer improved the strength of asphalt concrete against moisture damage, especially in specimens made of granite aggregates.
2. Adding SBR polymer increases the cohesion and adhesion free energy and reduces the debonding energy in stripping of specimens containing both types of aggregates, which indicates a decrease in the tendency of the system for stripping.
3. The stripping percentage index that is obtained by combining the results of the repetitive loading test in wet and dry conditions along with the results of the thermodynamic parameters indicate that the specimens made of controlled asphalt binders in loading cycles under wet conditions are subject to a higher rate of stripping, and the falling rate of the loading modulus in them is faster than the modified specimens.
4. The use of SBR polymer has increased both the basic and acidic components of asphalt binders. The percentage of increase in the basic component is higher than the acidic component, which results in the formation of more basic properties in the asphalt binders modified by this material.
5. Adding SBR polymer has increased the asphalt binder's polar component. The positive or negative impact of this parameter on the asphalt binder aggregates adhesion cannot be stated with certainty. The only thing to note is that the increase in the polar properties of asphalt binders increases the desire of its adhesion to polar materials such as aggregates and water.
6. The use of SBR polymer has increased the non-polar component of the modified asphalt binders compared to the base asphalt binder. This leads to the formation of stronger non-polar bonds.

#### References

1. Arabani, M., Shabani, A., Hamed, G.H. Experimental Investigation of Effect of Ceramic Fibers on Mechanical Properties of Asphalt Mixtures. *Journal of Materials in Civil Engineering*. 2019. 31 (9). DOI: 10.1061/(ASCE)MT.1943-5533.0002821
2. Shekhovtsova, Sy., Korolev, E., Inozemtcev, S., Yu, J., Yu, H. Method of forecasting the strength and thermal sensitive asphalt concrete. *Magazine of Civil Engineering*. 2019. 89 (5). Pp. 129–140. DOI: 10.18720/MCE.89.11

3. Stuart, K. Moisture damage in asphalt mixtures-a state-of-the-art report. 1990. Pp. 125. URL: <https://trid.trb.org/view/1175602> (date of application: 16.12.2019).
4. McGennis, R.B., Kennedy, T.W., Machemehl, R.B. Stripping and moisture damage in asphalt mixtures. Center For Transportation Research, The University Of Texas, Austin. 1984.
5. Hamed, G.H. Evaluating the effect of asphalt binder modification using nanomaterials on the moisture damage of hot mix asphalt. Road Materials and Pavement Design. 2017. 18 (6). Pp. 1375–1394. DOI: 10.1080/14680629.2016.1220865
6. Al-Qadi, I.L., Abuawad, I.M., Dhasmana, H., Coenen, A.R., Trepanier, J.S. Effects of Various Asphalt Binder Additives/Modifiers on Moisture-Susceptible Asphaltic Mixtures. Illinois Center for Transportation. 2014.
7. Zavyalov, M.A., Kirillov, A.M. Evaluation methods of asphalt pavement service life. Magazine of Civil Engineering. 2017. 70 (2). Pp. 42–56. DOI: 10.18720/MCE.70.5
8. Elphinstone, G. Adhesion and cohesion in asphalt-aggregate systems. Texas A&M University, 1998.
9. Cheng, D. Surface free energy of asphalt-aggregate system and performance analysis of asphalt concrete based on surface free energy. Texas A&M University, 2003.
10. Fallahi Abandansari, H., Modarres, A. Investigating effects of using nanomaterial on moisture susceptibility of hot-mix asphalt using mechanical and thermodynamic methods. Construction and Building Materials. 2017. 131. Pp. 667–675. DOI: 10.1016/j.conbuildmat.2016.11.052
11. Bhasin, A. Development of methods to quantify bitumen-aggregate adhesion and loss of adhesion due to water. Texas A&M University, 2006.
12. Howson, J.E. Relationship between surface free energy and total work of fracture of asphalt binder and asphalt binder-aggregate interfaces. Texas A&M University, 2011.
13. Hamed, G.H., Moghadas Nejad, F. Using energy parameters based on the surface free energy concept to evaluate the moisture susceptibility of hot mix asphalt. Road Materials and Pavement Design. 2015. 16 (2). Pp. 239–255. DOI: 10.1080/14680629.2014.990049
14. Hamed, G.H., Moghadas Nejad, F. Evaluating the effect of mix design and thermodynamic parameters on moisture sensitivity of hot mix asphalt. Journal of Materials in Civil Engineering. 2017. 29 (2). DOI: 10.1061/(ASCE)MT.1943-5533.0001734
15. Cai, L., Shi, X., Xue, J. Laboratory evaluation of composed modified asphalt binder and mixture containing nano-silica/rock asphalt/SBS. Construction and Building Materials. 2018. 172. Pp. 204–211. DOI: 10.1016/j.conbuildmat.2018.03.187
16. Moghadas Nejad, F., Azarhoosh, A.R., Hamed, G.H., Azarhoosh, M.J. Influence of using nanomaterial to reduce the moisture susceptibility of hot mix asphalt. Construction and Building Materials. 2012. 31. Pp. 384–388. DOI: 10.1016/j.conbuildmat.2012.01.004
17. Hamed, G.H., Moghadas Nejad, F., Oveisi, K. Investigating the effects of using nanomaterials on moisture damage of HMA. Road Materials and Pavement Design. 2015. 16 (3). Pp. 536–552. DOI: 10.1080/14680629.2015.1020850
18. Hamed, G.H., Moghadas Nejad, F. Use of aggregate nanocoating to decrease moisture damage of hot mix asphalt. Road Materials and Pavement Design. 2016. 17 (1). Pp. 32–51. DOI: 10.1080/14680629.2015.1056215
19. Moghadas Nejad, F., Arabani, M., Hamed, G.H., Azarhoosh, A.R. Influence of using polymeric aggregate treatment on moisture damage in hot mix asphalt. Construction and Building Materials. 2013. 47. Pp. 1523–1527. DOI: 10.1016/j.conbuildmat.2013.06.060
20. Hesami, S., Roshani, H., Hamed, G.H., Azarhoosh, A. Evaluate the mechanism of the effect of hydrated lime on moisture damage of warm mix asphalt. Construction and Building Materials. 2013. 47. Pp. 935–941. DOI: 10.1016/j.conbuildmat.2013.05.079
21. Faramarzi, M., Golestani, B., Lee, K.W. Improving moisture sensitivity and mechanical properties of sulfur extended asphalt mixture by nano-antistripping agent. Construction and Building Materials. 2017. 133. Pp. 534–542. DOI: 10.1016/j.conbuildmat.2016.12.038
22. Park, D.W., Seo, W.J., Kim, J., Vo, H.V. Evaluation of moisture susceptibility of asphalt mixture using liquid anti-stripping agents. Construction and Building Materials. 2017. 144. Pp. 399–405. DOI: 10.1016/j.conbuildmat.2017.03.214
23. Souliman, M.I., Hajj, E.Y., Sebaaly, P.E. Impact of antistripping additives on the long-term aging rheological properties of asphalt binders. Journal of Materials in Civil Engineering. 2015. 27(8). DOI:10.1061/(ASCE)MT.1943-5533.0001111.
24. ASTM D7369. Standard test method for determining the resilient modulus of bituminous mixtures by indirect tension test. West Conshohocken, PA, 2011.
25. De, S.K., White, J.R. Rubber technologist's handbook. Smithers Rapra Technology. New York, 2001.
26. Arabani, M., Shabani, A. Evaluation of the ceramic fiber modified asphalt binder. Construction and Building Materials. 2019. 205. Pp. 377–386. DOI: 10.1016/j.conbuildmat.2019.02.037
27. ASTM D1559. Test method for resistance of plastic flow of bituminous mixtures using marshall apparatus. West Conshohocken, PA, 1989.
28. Shah, B.D. Evaluation of moisture damage within asphalt concrete mixes. Texas A&M University, 2004.
29. Little, D.N., Bhasin, A. Using Surface Energy Measurements to Select Materials for Asphalt Pavement. National Cooperative Highway Research Program (NCHRP). 2006. 104.
30. Shekhovtsova, S.Y., Korotkov, A. V., Vysotskaya, M.A. Method of forecasting the effectiveness of cationic bitumen emulsions. Magazine of Civil Engineering. 2018. 78 (2). Pp. 91–100. DOI: 10.18720/MCE.78.7
31. Witczak, M., Kaloush, K., Pellinen, T., El-Basyouny, M. Appendix A–Test method for dynamic modulus of asphalt concrete mixtures for permanent deformation. National Cooperative Highway Research Program (NCHRP). 2002. 465.
32. Tarrer, A., Wagh, V. The effect of the physical and chemical characteristics of the aggregate on bonding. Strategic Highway Research Program (SHRP). 1991.
33. Hicks, R. Moisture damage in asphalt concrete, NCHRP synthesis of highway practice 175. Transportation Research Board. 1991.

### Contacts:

Amir Shabani, [amirsh@kth.se](mailto:amirsh@kth.se)

Gholam Hossein Hamed, [hamed@guilan.ac.ir](mailto:hamed@guilan.ac.ir)

Shabani, A., Hamed, Gh.H.